

Structured Inverted-File k-Means Clustering for High-Dimensional Sparse Data

Kazuo Aoyama and Kazumi Saito

Abstract—This paper presents an architecture-friendly k-means clustering algorithm called SIVF for a large-scale and high-dimensional sparse data set. Algorithm efficiency on time is often measured by the number of costly operations such as similarity calculations. In practice, however, it depends greatly on how the algorithm adapts to an architecture of the computer system which it is executed on. Our proposed SIVF employs invariant centroid-pair based filter (ICP) to decrease the number of similarity calculations between a data object and centroids of all the clusters. To maximize the ICP performance, SIVF exploits for a centroid set an inverted-file that is structured so as to reduce pipeline hazards. We demonstrate in our experiments on real large-scale document data sets that SIVF operates at higher speed and with lower memory consumption than existing algorithms. Our performance analysis reveals that SIVF achieves the higher speed by suppressing performance degradation factors of the number of cache misses and branch mispredictions rather than less similarity calculations.

Index Terms—Algorithm, Computer architecture, Data structure, High-dimensional sparse data, k-means clustering, Inverted file



1 INTRODUCTION

Machine learning algorithms are required to efficiently process huge data sets in many applications with increasing an amount of available data [1]. Such data sets are often high-dimensional sparse ones, which are ubiquitous, e.g., text (image or audio) data with bag-of-words (-visual or -acoustic words) representations [2], [3], [4], [5] and log data in computational advertising and recommender systems [6]. To design and implement an efficient algorithm for the data sets, it is important to leverage advantages of a modern computer system which the algorithm is executed on. In general, algorithm efficiency is measured by computational complexity on time and space regarding increasing input sizes so as to be platform-independent and instance-independent [7]. However, the relative merits of algorithms on speed performance may turn out to be different in practice from those evaluated based on the efficiency measure since their performance depends on characteristics of the data sets and the computer systems.

A modern computer system contains two main components: processors and a hierarchical memory system. A processor has several operating units each of which has deep pipelines with superscalar out-of-order execution and multilevel cache hierarchy [8]. The memory system consists of registers and multilevel caches in a processor and external memories such as a main memory and flash storages [9]. To efficiently operate an algorithm at high throughput in such a system, we must prevent *pipeline hazards*, which cause the pipeline stalls resulting in degrading the pipeline performance. A serious hazard is a control hazard induced by branch mispredictions [10], [11]. Another is a data hazard that can occur when data dependence exists between instructions. In particular, the data hazard caused by cache misses leads to serious performance degradation (e.g., [12]). To designing an *architecture-friendly* algorithm, we have to suppress both branch

mispredictions and cache misses.

To design an architecture-friendly algorithm for large-scale and high-dimensional sparse data sets, we consider a widely-used Lloyd-type k -means clustering algorithm [13] because the algorithm is one of fundamental machine learning algorithms and has been improved on speed performance by reducing costly similarity calculations based on the foregoing efficiency measure [14]. Lloyd's algorithm [15], [16], which is an iterative heuristic algorithm, partitions a given object data set into k subsets (clusters) with given positive integer k . By repeating two steps of an assignment and an update step until convergence from a given initial state, the algorithm locally minimizes an objective function, which is defined by the sum of the squared Euclidean distances between all pairs of an object feature vector and a mean feature vector of the cluster to which the object is assigned. Many accelerated Lloyd's algorithms have also been reported as described in Section 2.1.

There is a special Lloyd-type algorithm for a text data set, a spherical k -means algorithm [17]. Unlike the Lloyd's algorithm, the spherical k -means uses feature vectors normalized by their L_2 norms, i.e., points on a unit hypersphere, as an input data set and adopts a cosine similarity for a similarity measure between a pair of points. Each mean feature vector is also normalized by its L_2 norm. An objective function is defined by the sum of the cosine similarities between all the pairs of an object feature vector and a mean feature vector of the cluster to which the object is assigned. A solution by the spherical k -means coincides with that by the Lloyd's algorithm that uses the same feature vectors although their similarity and distance measures differ from each other. We employ the same settings as that of the spherical k -means to design our proposed algorithm dealing with high-dimensional sparse data sets like text data sets in Section 4.

Our challenge is to develop a high-performance Lloyd-type k -means clustering algorithm for a large-scale and high-dimensional sparse data set, exploiting advantages of the architecture in the modern computer system. We propose a structured inverted-file k -means clustering algorithm referred to as *SIVF*. Our proposed

-
- K. Aoyama is with NTT Communication Science Laboratories, Kyoto, Japan.
E-mail: kazuo.aoyama.rd@hco.ntt.co.jp
 - K. Saito is with Kanagawa University.
E-mail: k-saito@kanagawa-u.ac.jp

SIVF utilizes sparse expressions for both object and mean feature vectors for low memory consumption and applies an inverted-file data structure to the *mean* feature vectors. For high-speed performance, *SIVF* leverages an invariant centroid-pair based filter (ICP) that reduces similarity calculations. The inverted-file in *SIVF* has a special structure that enables the ICP to work efficiently, resulting in reducing branch mispredictions and last-level cache misses as shown in Sections 5 and 6.

Our contributions are threefold:

- 1) We present a simple yet efficient architecture-friendly k -means clustering algorithm, a structured inverted-file k -means clustering algorithm (*SIVF*), for a large-scale and high-dimensional sparse data set with potentially numerous classes in Section 4. Our proposed *SIVF* utilizes a structured inverted file for a set of mean feature vectors to make an invariant centroid-pair based filter (ICP) work efficiently.
- 2) We experimentally demonstrate that *SIVF* achieves superior performance on speed and memory consumption when it is applied to large-scale and high-dimensional real document data sets with large k values, comparing it with existing algorithms.
- 3) We analyze the *SIVF* performance with the *perf tool* [18]. The analysis reveals that *SIVF*'s high speed is clearly attributed to two main factors: fewer cache misses and fewer branch mispredictions. They are detailed in Sections 5 and 6.

The remainder of this paper consists of the following six sections. Section 2 briefly reviews related work from viewpoints that clarify the distinct aspects of our work. Section 3 describes preliminaries for understanding our proposed algorithm. Section 4 explains our proposed *SIVF* in detail. Section 5 shows our experimental settings and demonstrates the results. Section 6 discusses *SIVF*'s performance. The final section provides our conclusion.

2 RELATED WORK

Our algorithm is an accelerated Lloyd-type algorithm suitable to a large-scale sparse data set. This section reviews acceleration algorithms, followed by algorithms employing inverted-file structure for sparse data.

2.1 Acceleration Algorithms

A k -means clustering problem is defined as follows. Given a set of object feature vectors that are points in a D -dimensional Euclidean space, $\mathcal{X} = \{\mathbf{x}_1, \mathbf{x}_2, \dots, \mathbf{x}_N\}$, $|\mathcal{X}| = N$, $\mathbf{x}_i \in \mathbb{R}^D$, and a positive integer of k , a k -means clustering problem is a problem of finding a set of k clusters, $\mathcal{C}^* = \{C_1^*, C_2^*, \dots, C_k^*\}$:

$$\mathcal{C}^* = \arg \min_{\mathcal{C} = \{C_1, \dots, C_k\}} \left(\sum_{C_j \in \mathcal{C}} \sum_{\mathbf{x}_i \in C_j} \|\mathbf{x}_i - \boldsymbol{\mu}_j\|_2^2 \right), \quad (1)$$

where $\|\star\|_2$ denotes the L_2 norm of vector \star and $\boldsymbol{\mu}_j \in \mathbb{R}^D$ is the mean feature vector of cluster C_j . Solving Eq. (1) is difficult in practical use due to a high computational cost. Instead, Lloyd's algorithm [15], [16] finds a local minimum in an iterative heuristic manner. The algorithm repeats two steps of an assignment and an update step until the convergence or a predetermined termination condition is satisfied.

Algorithm 1: Lloyd-type algorithm at the r th iteration

Input: \mathcal{X} , $\mathcal{M}^{[r-1]} = \{\boldsymbol{\mu}_1^{[r-1]}, \dots, \boldsymbol{\mu}_k^{[r-1]}\}$, (k)
Output: $\mathcal{C}^{[r]} = \{C_1^{[r]}, C_2^{[r]}, \dots, C_k^{[r]}\}$, $\mathcal{M}^{[r]}$

- 1 $C_j^{[r]} \leftarrow \emptyset$, $j = 1, 2, \dots, k$
// Assignment step
- 2 **forall** $\mathbf{x}_i \in \mathcal{X}$ **do**
- 3 $d_{min} \leftarrow d(\mathbf{x}_i, \boldsymbol{\mu}_{a(\mathbf{x}_i)}^{[r-1]}) = \|\mathbf{x}_i - \boldsymbol{\mu}_{a(\mathbf{x}_i)}^{[r-1]}\|_2$
- 4 (I)
- 5 **forall** $\boldsymbol{\mu}_j^{[r-1]} \in \mathcal{M}^{[r-1]}$ **do**
- 6 if $d(\mathbf{x}_i, \boldsymbol{\mu}_j^{[r-1]}) < d_{min}$ **then**
- 7 $d_{min} \leftarrow d(\mathbf{x}_i, \boldsymbol{\mu}_j^{[r-1]})$ and $a(\mathbf{x}_i) \leftarrow j$
- 8 $C_{a(\mathbf{x}_i)}^{[r]} \leftarrow C_{a(\mathbf{x}_i)}^{[r]} \cup \{\mathbf{x}_i\}$
// Update step
- 9 $\boldsymbol{\mu}_j^{[r]} \leftarrow \left(\sum_{\mathbf{x}_i \in C_j^{[r]}} \mathbf{x}_i \right) / |C_j^{[r]}|$, $j = 1, 2, \dots, k$
- 10 (II)
- 11 **return** $\mathcal{C}^{[r]} = \{C_1^{[r]}, C_2^{[r]}, \dots, C_k^{[r]}\}$, $\mathcal{M}^{[r]}$

Algorithm 1 shows an overview of a Lloyd-type algorithm at the r th iteration. The assignment step assigns a point represented by object feature vector \mathbf{x}_i to cluster C_j whose centroid (mean at the previous iteration $\boldsymbol{\mu}_j^{[r-1]}$) is closest to \mathbf{x}_i . At line 3, d_{min} denotes a tentative minimum distance from \mathbf{x}_i to the centroids and $a(\mathbf{x}_i)$ is a function of \mathbf{x}_i that returns closest centroid ID j . The update step calculates mean feature vector $\boldsymbol{\mu}_j^{[r]} \in \mathcal{M}^{[r]}$ at the r th iteration using object feature vectors $\mathbf{x}_i \in C_j^{[r]}$.

Many acceleration algorithms have been reported [19], [20], [21], [22], [23], [24], [25]. We focus on their main filters and review the algorithms based on the triangle inequality, which are compared with our proposed *SIVF* in Section 5. We also describe an invariant centroid-pair based filter (ICP) [24], [26], [27] that *SIVF* leverages.

Main filters of Elkan's [19], Hamerly's [20], Drake's [21], and Ding's algorithm [22] are based on the same principle of skipping unnecessary distance calculations. Elkan's algorithm sets its main filter at line 4 (I) in Algorithm 1 as follows.

if $d(\mathbf{x}_i, \boldsymbol{\mu}_{a(\mathbf{x}_i)}^{[r-1]}) < d_{LB}(\mathbf{x}_i, \boldsymbol{\mu}_j^{[r-1]}) - \delta(\boldsymbol{\mu}_j^{[r-1]})$
then continue ,

where $d_{LB}(\mathbf{x}_i, \boldsymbol{\mu}_j^{[r-1]})$ denotes the lower bound on the distance between \mathbf{x}_i and $\boldsymbol{\mu}_j$ at the $(r-1)$ th iteration, i.e., $d(\mathbf{x}_i, \boldsymbol{\mu}_j^{[r-1]})$, and $\delta(\boldsymbol{\mu}_j^{[r-1]}) = d(\boldsymbol{\mu}_j^{[r-1]}, \boldsymbol{\mu}_j^{[r-2]})$. This algorithm needs the memory capacity of $O(N \cdot k)$ to store the distance lower bounds.

Hamerly's algorithm improves Elkan's on memory consumption from $O(N \cdot k)$ to $O(N)$ at the expense of a weaker filter. A main filter is set at line 4.

if $d(\mathbf{x}_i, \boldsymbol{\mu}_{a(\mathbf{x}_i)}^{[r-1]}) < d_{LB}(\mathbf{x}_i, \boldsymbol{\mu}_{2nd(\mathbf{x}_i)}^{[r-1]}) - \delta_{max}(\ast)$
then continue ,

where $\boldsymbol{\mu}_{2nd(\mathbf{x}_i)}^{[r-1]}$ is the second closest mean to \mathbf{x}_i at the $(r-1)$ th iteration and $\delta_{max}(\ast) = \max_{j \neq a(\mathbf{x}_i)} \delta(\boldsymbol{\mu}_j^{[r-1]})$.

Drake's and Ding's algorithm enhance filtering performance

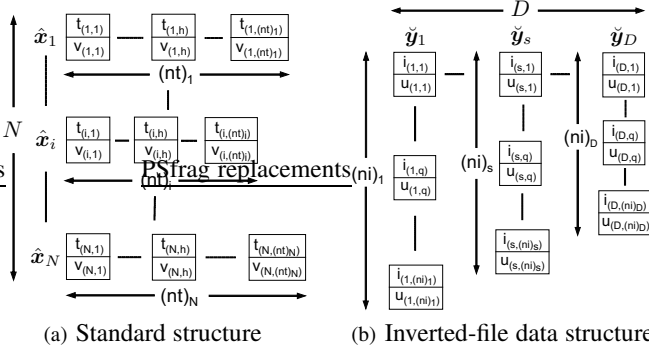


Fig. 1. Sparse expressions of feature vectors: (a) Object feature vector $\hat{x}_i = (t_{(i,h)}, v_{(i,h)})$ in standard structure where i denotes the global ID of objects ($i = 1, 2, \dots, N$) and h the local index of features ($h = 1, 2, \dots, (nt)_i$); (b) Object array \hat{y}_s that consists of tuples of object ID $i_{(s,q)}$ and feature $u_{(s,q)}$ in inverted-file data structure where s denotes the global ID of features ($s = 1, 2, \dots, D$) and q the local index of objects ($q = 1, 2, \dots, (ni)_s$).

using multiple distance lower bounds instead of only one for x_i in Hamerly’s algorithm. Drake’s algorithm uses b distance lower bounds ($1 < b < k$) between x_i and its b closest means. The first $(b - 1)$ lower bounds are determined in the same way as Elkan’s algorithm and the last one is done like Hamerly’s. Ding’s algorithm divides k means into g groups ($1 < g < k$) and uses one distance lower bound for each group. The lower bounds are obtained in the same manner as Hamerly’s. In the limits of $(b, g \rightarrow 1)$ and $(b, g \rightarrow k)$, the corresponding algorithms nearly approach Hamerly’s and Elkan’s algorithm, respectively. Both the filters are set at line 4. The lower bounds in the foregoing algorithms are updated at line 10 (II).

We select Drake’s and Ding’s algorithm as the algorithms compared with our *SIVF* due to their high performance. Before the comparison, we adapt them to sparse data sets in Section 3.1.

ICP omits the distance calculations between the μ_j and the x_i when $\delta(\mu_j^{[r-1]}) = 0$ and $\delta(\mu_{a(x_i)}^{[r-1]}) = 0$. ICP also saves the computational resources because of memory capacity of only $O(k)$ for Boolean flags that store whether $\mu_j^{[r-1]}$, $j = 1, \dots, k$, are invariant or not. We may relax the above restriction on x_i as $d(x_i, \mu_{a(x_i)}^{[r-1]}) \leq d(x_i, \mu_{a(x_i)}^{[r-2]})$ [27] if the memory capacity of $O(k+N)$ is allowed.

We incorporate ICP to an inverted-file based k -means clustering algorithm for acceleration. The inverted-file based algorithm is shown in Section 2.2 and a naïve acceleration algorithm is designed for comparison in Section 3.2.

2.2 Inverted-File Based Algorithms

When designing an algorithm for a sparse data set where each object is represented as a sparse feature vector, we have to carefully determine both a structure of the data set and an expression of the feature vector. Suppose that two object sets are given, each of which contains feature vectors normalized by their L_2 norms. The feature vector is a point on the unit hypersphere and a similarity between the feature vectors is measured by cosine similarity, i.e., their inner-product. When we calculate a similarity between feature vectors each of which has only several non-zero elements, we need to select a pair of a data structure and an expression of the object sets. The data structure is either a standard or an inverted-file one and the expression is either a full or a sparse one. A sparse

expression in a standard data structure is defined as a sequence of tuples of a feature ID ($t_{(i,h)}$) and a feature value ($v_{(i,h)}$) for each object in Fig. 1(a). By contrast, in an inverted-file data structure, an object array is defined as a sequence of tuples of an object ID ($i_{(s,q)}$) and the corresponding feature value ($u_{(s,q)}$) for each feature in Fig. 1(b).

In search algorithms for a text data set, a pair of a sparse expression and an inverted-file data structure is often adopted for invariant database that contains a set of object feature vectors [2], [28], [29], [30], [31] as in Fig. 1(b). Given query feature vector $\{\hat{x}_1\}$ represented with a sparse expression in a standard data structure in Fig. 1(a), a search algorithm identifies the $(nt)_1$ object arrays by the feature IDs of $t_{(1,h)}$, $h = 1, \dots, (nt)_1$, and calculates only the products of $v_{(1,h)}$ and $u_{(s,q)}$ where $s = t_{(1,h)}$ for their similarity. Thus it can find preferable documents quickly from the inverted-file database.

A k -means clustering algorithm processes both a data object set and a mean (centroid) set. If the data object set is a large-scale and high-dimensional sparse one, it is natural that the object feature vector is represented with a sparse expression. Furthermore, it is advisable that the mean feature vector is also represented with the sparse expression. In this situation, there are two usages of the inverted-file structure. One is to apply the inverted-file structure to an object data set [32]. The other is to do it to a mean set, which is referred to as *IVF*. Since the latter leads to higher performance than the former when applied to large-scale and high-dimensional real document data sets [33], we adopt the latter one for our proposed *SIVF* as in Section 4.

3 PRELIMINARIES

This section describes both a way for applying the acceleration algorithms in Section 2.1 to sparse data sets and a naïve method for accelerating inverted-file based k -means clustering algorithm by ICP. Our proposed algorithm is compared with the acceleration algorithms adapted with the former way and the algorithm made with the latter method.

3.1 Applying Accelerations to Sparse Data

Drake’s and Ding’s algorithm were originally designed for low-to moderate-dimensional dense data sets [21], [22] below 1,000 dimensions such as MNIST handwritten digit dataset (784 dimensions) [34] and 80 million tiny images (384 dimensions) [35]. We adapt them to a high-dimensional sparse data set whose dimensionality is over 100,000 and which has several non-zero elements. We assume that the standard data structure is applied to both an object data set and a mean set. It is natural that the object feature vectors are represented with the sparse expression because of the object data size and its sparsity as in Fig. 1(a). Then there are two choices to represent the mean feature vectors: the sparse and the full expression

Let us suppose that the mean feature vectors are represented with the sparse expression. This representation provides a positive effect on memory consumption while it causes speed-performance degradation. When both the object and the mean feature vectors employ the sparse expression in the standard data structure, i.e., each feature element in the vectors is a tuple of a feature ID and a feature value, an algorithm detects a pair of the tuples with an identical feature ID in the object and the mean feature vectors using many conditional branches. Since it is difficult to

Algorithm 2: Assignment step in *IVF* at r th iteration

Input: $\hat{\mathcal{X}}, \hat{\mathcal{M}}^{[r-1]}(k)$
Output: $\mathcal{C}^{[r]} = \{C_1^{[r]}, C_2^{[r]}, \dots, C_k^{[r]}\}$

- 1 $C_j^{[r]} \leftarrow \emptyset, j = 1, 2, \dots, k$
- 2 **foreach** $\hat{x}_i = (t_{(i,h)}, v_{(i,h)})_{h=1}^{(nt)_i} \in \hat{\mathcal{X}}$ **do**
- 3 $\rho_{max} \leftarrow 0, \boldsymbol{\rho} = (\rho_1, \rho_2, \dots, \rho_j, \dots, \rho_k) \leftarrow \mathbf{0}$
- 4 $S_i = \{t_{(i,1)}, t_{(i,2)}, \dots, t_{(i,h)}, \dots, t_{(i,(nt)_i)}\}$
- 5 **forall** $s \leftarrow t_{(i,h)} \in S_i$ **do**
- 6 // $\check{\xi}_s^{[r-1]} = [(c_{(s,q)}, u_{(s,q)})_{q=1}^{(mf)_s}]^{[r-1]}$
- 7 **forall** $(c_{(s,q)}, u_{(s,q)})^{[r-1]} \in \check{\xi}_s^{[r-1]}$ **do**
- 8 $\rho_{c_{(s,q)}} \leftarrow \rho_{c_{(s,q)}} + v_{(i,h)} \times u_{(s,q)}$
- 9 **for** $j \leftarrow 1$ **to** k **do**
- 10 **if** $\rho_j > \rho_{max}$ **then** $\rho_{max} \leftarrow \rho_j$ and $a(\hat{x}_i) \leftarrow j$
- 11 $C_{a(\hat{x}_i)}^{[r]} \leftarrow C_{a(\hat{x}_i)}^{[r]} \cup \{\hat{x}_i\}$
- 12 **return** $\mathcal{C}^{[r]}$

predict truth values of the conditions in most cases, a lot of branch mispredictions occur, resulting in the performance degradation.

In the case of the full expression, the foregoing conditional branches are unnecessary. A feature vector represented with the full expression is a sequence of D feature values arranged in ascending order of feature ID from 1 to D . If a feature value at a feature ID does not exist, zero-padding is performed at the ID. For this expression, an algorithm can directly access a feature value in the mean feature vector by using the object feature ID. We adopt the full expression for the mean feature vectors to adapt Drake's and Ding's algorithm to high-dimensional sparse data sets although this expression has the drawbacks of the requirement of a large amount of memory capacity and the possibility of decreasing an effective cache-hit rate.

3.2 Accelerating Inverted-File k-Means

Algorithm 2 shows a pseudocode of the assignment step at r th iteration in *IVF* [33]. Similarities are calculated in the triple loop at lines 2 to 7, where $\check{\xi}_s^{[r-1]}$ and $(mf)_s$ are the s th mean (centroid) array and the maximum of the s th local index that correspond to \check{y}_s and $(ni)_s$ in Fig. 1(b), respectively. *IVF* calculates similarities between object \hat{x}_i and only the limited centroids listed in centroid arrays $\check{\xi}_s^{[r-1]}$. On the negative side, the listed centroids are always the targets of similarity calculations without any filters.

To reduce the similarity calculations like other acceleration algorithms, we try to incorporate the invariant centroid-pair based filter (ICP) to *IVF*. Other acceleration algorithms based on the triangle inequality directly use the relationship between an object and a centroid while ICP exploits the relationship between a pair of centroids as shown in Section 2.1. That is, ICP does not calculate the similarity between $\boldsymbol{\mu}_j^{[r-1]}$ of $\delta(\boldsymbol{\mu}_j^{[r-1]}) = 0$ and \hat{x}_i of $\delta(\boldsymbol{\mu}_j^{[r-1]}) = 0$. We prepare a Boolean flag $\lambda_j, j = 1, \dots, k$ for each centroid, which is 1 if $\delta(\boldsymbol{\mu}_j^{[r-1]}) = 0$, otherwise 0. A naïve way to design *IVF* with ICP is to use two conditional branches based on the Boolean flag.

Algorithm 3 shows a part of the assignment step in *IVF* with ICP using conditional branches referred to as *IVF-CBICP*, which corresponds to lines 2 to 7 in Algorithm 2. Just before the second inner-most loop at line 4, the Boolean flag $\lambda_{a(\hat{x}_i)}^{[r-1]}$

Algorithm 3: *IVF-CBICP*: Part of assignment step

- 1 **foreach** $\hat{x}_i = (t_{(i,h)}, v_{(i,h)})_{h=1}^{(nt)_i} \in \hat{\mathcal{X}}$ **do**
- 2 $\rho_{max} \leftarrow 0, \boldsymbol{\rho} = (\rho_1, \rho_2, \dots, \rho_j, \dots, \rho_k) \leftarrow \mathbf{0}$
- 3 $S_i = \{t_{(i,1)}, t_{(i,2)}, \dots, t_{(i,h)}, \dots, t_{(i,(nt)_i)}\}$
- 4 **if** $\lambda_{a(\hat{x}_i)}^{[r-1]} = 1$ **then**
- 5 **forall** $s \leftarrow t_{(i,h)} \in S_i$ **do**
- 6 // $\check{\xi}_s^{[r-1]} = [(c_{(s,q)}, u_{(s,q)})_{q=1}^{(mf)_s}]^{[r-1]}$
- 7 **for** $q \leftarrow 1$ **to** $(mf)_s$ **do**
- 8 **if** $\lambda_{c_{(s,q)}}^{[r-1]} = 0$ **then**
- 9 $\rho_{c_{(s,q)}} \leftarrow \rho_{c_{(s,q)}} + v_{(i,h)} \times u_{(s,q)}$
- 10 **else**
- 11 **forall** $s \leftarrow t_{(i,h)} \in S_i$ **do**
- 12 **for** $q \leftarrow 1$ **to** $(mf)_s$ **do**
- 13 $\rho_{c_{(s,q)}} \leftarrow \rho_{c_{(s,q)}} + v_{(i,h)} \times u_{(s,q)}$

is evaluated. If the flag's value is 1, i.e., the cluster which \hat{x}_i belongs to is invariant, only the moving centroids are targets for the similarity calculations. The centroids are selected with the conditional branch in the inner-most loop at line 7. Thus *IVF-CBICP* utilizes ICP with two conditional branches. Although *IVF-CBICP* successfully reduced similarity calculations, it got little improvement on the speed performance as detailed in Section 6.

4 PROPOSED ALGORITHM: SIVF

We propose a structured inverted-file k -means clustering algorithm (*SIVF*). This algorithm was designed to efficiently process a large-scale and high-dimensional sparse data set at high speed and with low memory consumption, in particular, when a large k value is given, i.e., under a tough condition where any algorithms need a lot of computational resources. First, we adopted an inverted-file data structure for a centroid (mean) set [33] to leverage a physical memory effectively. Second, we incorporated an invariant centroid-pair based filter (ICP) [24], [26], [27] to reduce a computational cost by skipping unnecessary similarity calculations. Last, to combine ICP with a tentative algorithm using the inverted file, we gave the inverted file a special structure, which enables *SIVF* to exploit ICP without the conditional branch at line 7 in Algorithm 3. The structured inverted file consists of two parts: the front and the back part contain moving and invariant centroids, respectively. By replacing the end point of $(mf)_s$ at line 7 in Algorithm 3 with an index at the boundary of the foregoing two parts, we can remove the conditional branch. The pseudocode is shown in Algorithms 4 and 5.

4.1 Assignment Step

Algorithm 4 shows the assignment step in *SIVF* at the r th iteration. From the results at the $(r-1)$ th iteration, *SIVF* receives a centroid set and a Boolean-flag vector. The centroid set, which is the mean set at the $(r-1)$ th iteration, is represented with structured inverted-file sparse expression $\hat{\mathcal{M}}^{*[r-1]}$. The Boolean-flag vector $\boldsymbol{\lambda}^{[r-1]}$ consists of k elements $\lambda_j^{[r-1]}, j = 1, 2, \dots, k$. $\lambda_j^{[r-1]} = 1$ if the members in the j th cluster are invariant between the $(r-2)$ th and

Algorithm 4: *SIVF* assignment step at the r th iteration

Input: $\hat{\mathcal{X}}, \check{\mathcal{M}}^{*[r-1]}, \lambda^{[r-1]} = (\lambda_1^{[r-1]}, \dots, \lambda_k^{[r-1]})$, (k)
Output: $\mathcal{C}^{[r]} = \{C_1^{[r]}, C_2^{[r]}, \dots, C_k^{[r]}\}$, $\lambda^{[r]}$

- 1 $C_j^{[r]} \leftarrow \emptyset, j = 1, 2, \dots, k$
- 2 **do in parallel**
 - // Calculate similarities
 - 3 **foreach** $\hat{x}_i = (t_{(i,h)}, v_{(i,h)})_{h=1}^{(nt)_i} \in \hat{\mathcal{X}}$ **do**
 - 4 $\rho_{max} \leftarrow 0, \rho = (\rho_1, \rho_2, \dots, \rho_j, \dots, \rho_k) \leftarrow \mathbf{0}$
 - 5 $S_i = \{t_{(i,1)}, t_{(i,2)}, \dots, t_{(i,h)}, \dots, t_{(i,(nt)_i)}\}$
 - 6 **if** $\lambda_{a(\hat{x}_i)}^{[r-1]} = 1$ **then**
 - 7 **forall** $s \leftarrow t_{(i,h)} \in S_i$ **do**
 - 8 $\check{\xi}_s^{*[r-1]} = [(c_{(s,q)}, u_{(s,q)})_{q=1}^{(mf)_s}]^{*(r-1)}$
 - 9 **for** $q \leftarrow 1$ **to** $(mf_{[0]})_s$ **do**
 - 10 $\rho_{c_{(s,q)}} \leftarrow \rho_{c_{(s,q)}} + v_{(i,h)} \times u_{(s,q)}$
 - 11 **else**
 - 12 **forall** $s \leftarrow t_{(i,h)} \in S_i$ **do**
 - 13 $\rho_{c_{(s,q)}} \leftarrow \rho_{c_{(s,q)}} + v_{(i,h)} \times u_{(s,q)}$
 - 14 // Assign \hat{x}_i to a cluster
 - 15 **for** $j \leftarrow 1$ **to** k **do**
 - 16 **if** $\rho_j > \rho_{max}$ **then** $\rho_{max} \leftarrow \rho_j$ and $a(\hat{x}_i) \leftarrow j$
 - 17 $C_{a(\hat{x}_i)}^{[r]} \leftarrow C_{a(\hat{x}_i)}^{[r]} \cup \{\hat{x}_i\}$
- 18 // Mark invariant clusters
- 19 $\lambda^{[r]} \leftarrow \mathbf{0}$
- 20 **forall** $C_j^{[r]} \in \mathcal{C}^{[r]}$ **do**
- 21 **if** $C_j^{[r]} = C_j^{[r-1]}$ **then** $\lambda_j^{[r]} \leftarrow 1$
- 22 **return** $\mathcal{C}^{[r]}, \lambda^{[r]} = (\lambda_1^{[r]}, \dots, \lambda_k^{[r]})$

the $(r-1)$ th iteration, otherwise $\lambda_j^{[r-1]} = 0$. *SIVF* also uses a data object set represented with standard sparse expression $\hat{\mathcal{X}}$. At the assignment step, each cluster $C_j^{[r]}$ and Boolean-flag vector $\lambda_j^{[r]}$ are generated.

The triple loop at lines 3 to 13 and the assignment of an object to a cluster at lines 14 to 16 are executed by multithread processing. At the outer-most loop, the i th object feature vector ($\hat{x}_i \in \hat{\mathcal{X}}$) is chosen to determine a cluster which the i th object belongs to. \hat{x}_i consists of $(nt)_i$ tuples $(t_{(i,h)}, v_{(i,h)})$, $h = 1, 2, \dots, (nt)_i$, where $(nt)_i$ denotes the number of distinct terms that the i th object uses, h is the local counter, $t_{(i,h)}$ is the global feature ID (term ID) from 1 to D , and $v_{(i,h)}$ is the corresponding feature value such as *tf-idf*.

We insert the conditional branch just before the inner double loop at line 6 to identify whether the cluster $C_{a(\hat{x}_i)}^{[r-1]}$ which the i th object belongs to is invariant or not. If the cluster is invariant, we calculate similarities of the i th object to only the moving centroids that change their positions due to the changes of the cluster members, otherwise we have to do the similarities to all the centroids. This is ICP function of skipping the similarity calculations. To exploit the foregoing ICP, we give inverted-file centroid array $\check{\xi}_s^{*[r-1]}$ a simple but effective structure, where the moving centroids are placed at the front part indexed by 1

to $(mf_{[0]})_s$ in $\check{\xi}_s^{*[r-1]}$. This centroid array $\check{\xi}_s^{*[r-1]}$ consists of $(mf)_s$ tuples $(c_{(s,q)}, u_{(s,q)})^{*[r-1]}$, $q = 1, 2, \dots, (mf)_s$, where $c_{(s,q)}$ denotes the global centroid ID from 1 to k , $u_{(s,q)}$ is the corresponding value, and $(mf)_s$ denotes the centroid (mean) frequency of term ID s . Note that the centroid array is partitioned into two parts of the front ($1 \leq q \leq (mf_{[0]})_s$) and the back part ($(mf_{[0]})_s < q \leq (mf)_s$). Owing to the structured inverted-file centroid array, we can realize the ICP function only to specify the end position of the inner-most loop without the conditional branch. A partial similarity (corresponding to a partial inner product) of the i th object to the $c_{(s,q)}$ th centroid is calculated and stored at $\rho_{c_{(s,q)}}$ at lines 9 and 13.

Just after the inner double loop has been completed, the i th object is assigned to the $a(\hat{x}_i)$ th cluster whose centroid most closely resembles at lines 14 to 16. For the next iteration, we mark invariant clusters at lines 17 to 19. Last, the assignment step passes the cluster set $\mathcal{C}^{[r]}$ and the Boolean-flag vector $\lambda^{[r]}$ to the following update step.

4.2 Update Step

Algorithm 5 shows the update step at the r th iteration. At the update step, we calculate each mean of k clusters based on the object assignment and make a structured inverted file $\check{\mathcal{M}}^{*[r]}$ that consists of D inverted-file mean arrays $\check{\xi}_p^{*[r]}$, $p = 1, 2, \dots, D$.

We first determine both the length $(mf)_p$ and the end position $(mf_{[0]})_s$ of the inverted-file mean array $\check{\xi}_p^{*[r]}$, $p = 1, 2, \dots, D$ at lines 1 to 14. According to the element $\lambda_j^{[r]}$ in the Boolean-flag vector, we separately enumerate the numbers of moving and invariant means that contains the s th term and store those in $(mf_{[0]})_s$ and $(mf_{[1]})_s$, respectively.

We initialize two local counters, $q_{[0]p}$ for moving means and $q_{[1]p}$ for invariant means, in the p th inverted-file mean array $\check{\xi}_p^{*[r]}$, where p denotes the global term ID. Next, we calculate a mean feature vector in each cluster $C_j^{[r]}$ at lines 17 to 20. Based on an evaluation result of $\lambda_j^{[r]}$ in the Boolean-flag vector, we place both cluster ID (mean ID) and its feature value to an appropriate position in the inverted-file mean array at lines 21 to 30. Thus we complete structured inverted-file $\check{\mathcal{M}}^{*[r]}$ that consists of $\check{\xi}_p^{*[r]}$, $p = 1, \dots, D$.

SIVF utilizes a structured inverted file for a centroid set, which fuses ICP that skips unnecessary similarity calculations with an ordinary inverted file suitable to processing a large-scale sparse data set. Therefore, we can expect that *SIVF* efficiently works for a large-scale and high-dimensional sparse data set with low memory consumption and at high speed. In the following section, we qualitatively evaluate the *SIVF* performance, comparing it with existing algorithms.

5 EXPERIMENTS

We first describe data sets used in our experiments, a platform including a computer system where the algorithms were executed, and performance measures for evaluation. Next, we compare our proposed *SIVF* with existing algorithms regarding performance and analyze their performances with the *perf tool* [18]. We experimentally demonstrate that *SIVF* is superior to the existing algorithms when applied to high-dimensional sparse data sets.

Algorithm 5: *SIVF* update step at the r th iteration

Input: $\hat{\mathcal{X}}, \mathcal{C}^{[r]}, \lambda^{[r]}$
Output: $\check{\mathcal{M}}^{*[r]} = (\check{\xi}_1^{*[r]}, \check{\xi}_2^{*[r]}, \dots, \check{\xi}_p^{*[r]}, \dots, \check{\xi}_D^{*[r]})$

```

// Determine an inverted-file structure
1  $\mathbf{mf}_{[0]} = ((mf_{[0]})_1, \dots, (mf_{[0]})_D) \leftarrow \mathbf{0}$ 
2  $\mathbf{mf}_{[1]} = ((mf_{[1]})_1, \dots, (mf_{[1]})_D) \leftarrow \mathbf{0}$ 
3 for  $j \leftarrow 1$  to  $k$  do
4   if  $\lambda_j^{[r]} = 0$  then
5     forall  $C_j^{[r]} \in \mathcal{C}^{[r]}$  do
6        $S_\mu \leftarrow \emptyset$  // Tentative term ID set
7       forall  $\hat{x}_i \in C_j^{[r]}$  do  $S_\mu \leftarrow S_\mu \cup \{t_{(i,h)} \in S_i\}$ 
8       forall  $s \in S_\mu$  do  $(mf_{[0]})_s \leftarrow (mf_{[0]})_s + 1$ 
9   else
10    forall  $C_j^{[r]} \in \mathcal{C}^{[r]}$  do
11       $S_\mu \leftarrow \emptyset$  // Tentative term ID set
12      forall  $\hat{x}_i \in C_j^{[r]}$  do  $S_\mu \leftarrow S_\mu \cup \{t_{(i,h)} \in S_i\}$ 
13      forall  $s \in S_\mu$  do  $(mf_{[1]})_s \leftarrow (mf_{[1]})_s + 1$ 
14 for  $p \leftarrow 1$  to  $D$  do  $(mf)_p \leftarrow (mf_{[0]})_p + (mf_{[1]})_p$ 
// Make structured inverted-file  $\check{\mathcal{M}}^{*[r]}$ 
15  $q_{[0]p} \leftarrow 1, \boxed{q_{[1]p} \leftarrow (mf_{[0]})_p + 1}, p = 1, 2, \dots, D$ 
16 forall  $C_j^{[r]} \in \mathcal{C}^{[r]}$  do
// Calculate mean features
17  $\mathbf{w} = (w_1, \dots, w_D) \leftarrow \mathbf{0}$  // Tentative vector
18 forall  $\hat{x}_i \in C_j^{[r]}$  do
19   forall  $s \leftarrow t_{(i,h)} \in S_i$  do  $w_s \leftarrow w_s + v_{(i,h)}$ 
20 for  $p \leftarrow 1$  to  $D$  do  $w_p \leftarrow w_p / |C_j^{[r]}|$ 
// Make inverted-file mean arrays
21 if  $\lambda_j^{[r-1]} = 0$  then
22   for  $p \leftarrow 1$  to  $D$  do
23     if  $w_p \neq 0$  then
24        $c_{(p,q_{[0]p})} \leftarrow j, u_{(p,q_{[0]p})} \leftarrow w_p / \|\mathbf{w}\|_2$ 
25        $q_{[0]p} \leftarrow q_{[0]p} + 1$ 
26   else
27     for  $p \leftarrow 1$  to  $D$  do
28       if  $w_p \neq 0$  then
29          $c_{(p,q_{[1]p})} \leftarrow j, u_{(p,q_{[1]p})} \leftarrow w_p / \|\mathbf{w}\|_2$ 
30          $q_{[1]p} \leftarrow q_{[1]p} + 1$ 
31 return  $\check{\mathcal{M}}^{*[r]}$ 

```

5.1 Data Sets

We employed two different types of large-scale and high-dimensional sparse real document data sets: *PubMed Abstracts* (PubMed for short) [36] and *The New York Times Articles* (NYT).

The PubMed data set contains 8,200,000 documents (texts) each of which was represented by the term (distinct word) counts. We made a feature vector normalized by its L_2 norm from each document, which consisted of the *tf-idf* values of the corresponding terms. Each feature vector was regarded as a point on a unit hypersphere. We made five data sets that were referred to as 500K, 1M, 2M, 5M, and 8M-sized PubMed. The N -sized PubMed had N feature vectors chosen at random without duplication

from all of the vectors, e.g., 1M-sized PubMed had 1,000,000 feature vectors. The data sets contained distinct terms (vocabulary) corresponding to dimensionality of 139,845, 140,914, 141,041, 141,043, and 141,043 in ascending order of data size. The average term frequencies in the documents, i.e., the average numbers of non-zero elements in the feature vectors, were 58.96, 58.95, 58.97, 58.96, and 58.96 in the same order.

We extracted 1,285,944 articles from NYT from 1994 to 2006 and counted the frequency of the term occurrences after stemming and stop word removal. In the same manner as PubMed, we made a set of feature vectors with 495,714 dimensionality. The average number of non-zero elements in the feature vectors was 225.76. Thus both the data sets are large-scale and high-dimensional sparse ones.

5.2 Platform and Measures

All the algorithms were executed on a computer system that was equipped with two Xeon E5-2697v3 2.6-GHz CPUs with three-level caches from levels 1 to level 3 (last level) [37] and a 256-GB main memory, by multithreading with OpenMP [38] within the memory capacity. In the CPU, the out-of-order superscalar execution was performed with eight issue widths and the last-level cache has 36,700,160 (35M) bytes consisting of 64-byte blocks with 20-way set associative placement and least-recently used (LRU) replacement [37], [39]. The algorithms were implemented in C and compiled with a GNU C compiler (gcc) version 8.2.0 on the optimization level of `-O3`. The performances of the algorithms were evaluated with CPU time (or clock cycles) until convergence and the maximum size of the physical memory occupied through the iterations. To analyze the speed performance, we measured *performance degradation factors* with the *perf tool* (Linux profiling with performance counters) [18]. In particular, we focused on the number of completed instructions (Inst for short), branch mispredictions (BM), and last-level cache misses (LLCM).

5.3 Performance Evaluation

First, we compared *SIVF* with two existing algorithms of Drake's (*Drake*⁺) [21] and Ding's (*Ding*⁺) [22] algorithm and our designed *Lloyd-ICP*, which was a modified Lloyd's algorithm incorporating ICP as a baseline. The three compared algorithms were implemented with the method shown in Section 3.1. That is, each mean feature vector was represented as a vector with full dimensionality. Next, we analyzed *SIVF* speed performance, focusing on the number of similarity calculations and the performance degradation factors (DFs). The evaluation results showed that *SIVF* was superior to the compared algorithms in PubMed and NYT. The high speed came from the suppression of DFs rather than less similarity calculations. Our results in PubMed is shown here and those in NYT is done in Appendix A.

5.3.1 Comparison with existing algorithms

Figures 2(a) and (b) show that each of the four algorithms required average elapsed time per iteration and maximum physical memory size through iterations until convergence when they were executed by 50-thread processing with OpenMP in 1M-sized PubMed, given the k values of (1,000, 2,000, 5,000, 10,000, 20,000). As shown in Section 2.1, the compared Ding's and Drake's algorithm have parameters g and b , respectively. These parameters were set at $k/10$ as shown in [22]. The average elapsed time of *SIVF* slowly increased with k and was much smaller than the others'

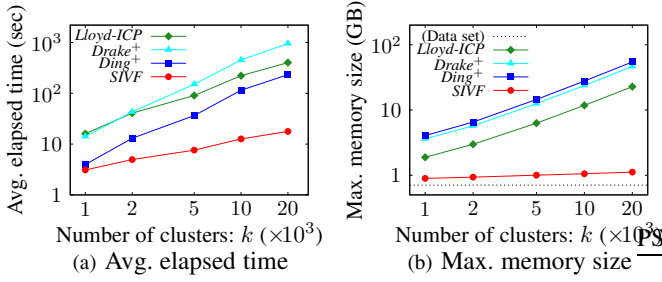


Fig. 2. Performance of four algorithms executed by 50-thread processing with given k in 1M-sized PubMed. (a) Average elapsed time per iteration and (b) Occupied maximum physical memory size through iterations are plotted along k with log-log scale.

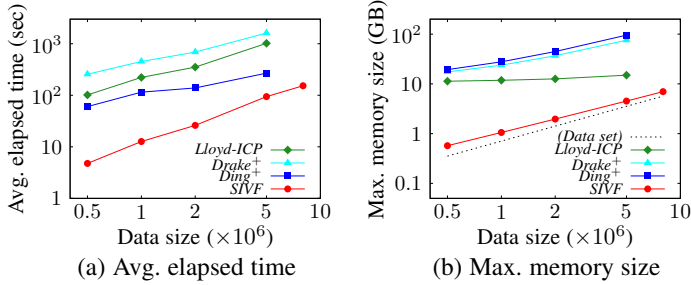


Fig. 3. Performance of four algorithms executed by 50-thread processing for PubMed with different sizes when $k=10,000$. (a) Average elapsed time per iteration and (b) Occupied maximum memory size through iterations are plotted along data size with log-log scale.

in the large k region of $k \geq 2,000$, in particular, it was only 7.6% of that required by *Ding*⁺ at $k = 20,000$. This k region is a tough condition where the algorithms except *SIVF* needed so much computational time. Regarding memory consumption, *SIVF* used small memory sizes in all the k values because of its sparse feature vector representation of both the data object and mean sets.

Figures 3(a) and (b) show the average elapsed time per iteration and the maximum physical memory size that each of the four algorithms required with data size N when the algorithms were executed in N -sized PubMed at $k = 10,000$ by 50-thread processing, where $N = (5 \times 10^5, 1 \times 10^6, 2 \times 10^6, 5 \times 10^6, 8 \times 10^6)$. *SIVF* achieved the best performance among the algorithms. The algorithms except *SIVF* did not work for 8M-sized PubMed.

5.3.2 Performance analysis

To analyze the speed performance of the algorithms, we focused on the results in 1M-sized PubMed, given $k = 20,000$, where the marked performance differences were found.

Figure 4 shows that the elapsed times that the four algorithms required at each iteration from the start to the convergence (through 32 iterations) when they were executed by 50-thread processing. We notice that *SIVF* operated much faster than the others. The elapsed time of *SIVF* was only 568 sec while that of the second fastest *Ding*⁺ was 7440 sec.

Figure 5 shows the filter performance of each algorithm, i.e., the ability of skipping unnecessary similarity calculations at each iteration. The filter performance was evaluated by a rate of the number of similarity calculations to $(N \times k)$, which corresponds to that required by Lloyd's algorithm, and is illustrated along iteration with linear-log scale. When a filter works better, its rate becomes smaller. We notice that the filter of *Ding*⁺ reduced more similarity calculations, which is an indicator of a computational cost, than the others'. Why did *Ding*'s algorithm equipped with

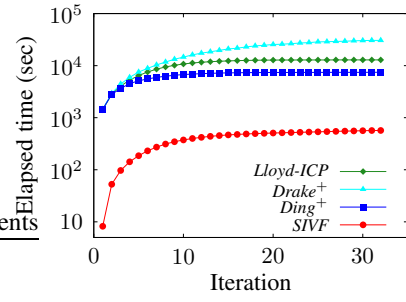


Fig. 4. Elapsed time that four algorithms with $k=20,000$ required until convergence when they were executed by 50-thread processing for 1M-sized PubMed. Elapsed time is plotted along iteration with linear-log scale.

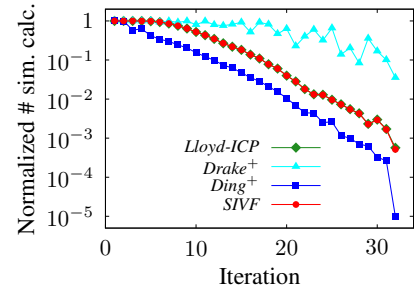


Fig. 5. Number of similarity calculations normalized by $(N \times k)$ per iteration, where N indicates the data size of 1M, when four algorithms with $k=20,000$ were executed by 50-thread processing for 1M-sized PubMed. Normalized number is plotted along iteration with linear-log scale.

the high-performance filter need more elapsed time than *SIVF* as shown in Fig. 4?

We demonstrate that the elapsed time that an algorithm needs at run-time crucially depends on not only the number of expensive similarity calculations but also the performance degradation factors (DFs) related to a computer architecture. Figure 6(a) shows the average number of similarity calculations per iteration that is normalized by $(N \times k)$ when the four algorithms varying k were executed by 50-thread processing for 1M-sized PubMed. It is clear that the *Ding*'s algorithm (*Ding*⁺) remarkably reduced the similarity calculations in all k range. Note that the performances in Fig. 5 correspond to the points at $k = 20,000$ in Fig. 6(a). Figures 6(b), (c), and (d) show the characteristics of DFs, the number of (b) retired (successfully completed) instructions (Inst), (c) branch mispredictions (BM), and (d) last-level cache misses (LLCM). The numbers of retired instructions of the three algorithms except *Drake*⁺ were within one order of magnitude in Fig. 6(b). By contrast, BM and LLCM of *SIVF* were extremely small, compared with those of the others. In particular, at $k = 20,000$, the rates of *SIVF*'s BM and LLCM to *Ding*⁺'s were 0.47% and 0.95%, respectively. Since penalties of a branch misprediction and a last-level cache miss substantially delay the process [10], [11], [33], [40], the foregoing differences in DFs have a severe impact on the elapsed time. In fact, the penalty of clock cycles becomes several tens to several hundreds times as high as the number of clock cycles per retired instruction in a modern computer system with out-of-order superscalar execution.

Thus architecture-friendly *SIVF* achieved the high-speed performance by suppressing the DFs rather than less similarity calculations. In the following section, we discuss the effect of giving an appropriate structure to a data set, i.e., a structured

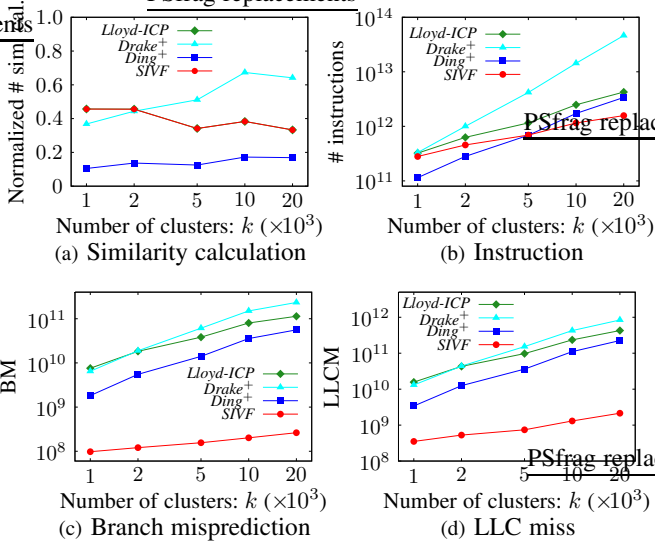


Fig. 6. (a) Average number of similarity calculations normalized by $(N \times k)$ until the convergence and characteristics of performance degradation factors: (b) the number of instructions, (c) branch mispredictions (BM), and (d) last-level cache misses (LLCM) when the three algorithms were executed by 50-thread processing for 1M-sized PubMed. (a) is plotted with log-linear scale and (b), (c), and (d) with log-log scale.

inverted file for a mean set, comparing *SIVF* with *IVF-CBICP* using an unstructured inverted file in Section 3.2.

6 DISCUSSION

We detail a positive effect of the structured inverted file on the elapsed time, comparing *SIVF* with two prepared algorithms: One is baseline algorithm *IVF* employing only an inverted-file for a mean (centroid) set without ICP. The other is naïve algorithm *IVF-CBICP* that utilizes ICP with a conditional branch shown in Section 3.2. Since inverted-file mean array $\xi_s^{[r-1]}$ in *IVF-CBICP* has no structure, all the centroids $c_{(s,q)}$, $1 \leq q \leq (mf)_s$, are evaluated at the inner-most loop in lines 6 to 8 in Algorithm 3 whether a similarity calculation between the $c_{(s,q)}$ th centroid and the i th object is necessary or not using the conditional branch at line 7 in Algorithm 3.

Figure 7 shows the performance of the three algorithms that were executed by 50-thread processing in 1M-sized PubMed, given k values. The maximum physical memory sizes used by the algorithms were almost the same in all the k range in Fig. 7(b) because the algorithms did not have much difference in their object and mean data sizes. In terms of the speed performance in Fig. 7(a), *SIVF* operated faster than the others and the performance difference increased with k . This difference between *SIVF* and *IVF-CBICP* came from the structure of the inverted-file arrays.

We first observe the number of similarity calculations before discussing the effects of the DFs. Figure 8(a) shows that the number of similarity calculations normalized by $(N \times k)$. The baseline algorithm, *IVF* without ICP, performed all the similarity calculations like Lloyd’s algorithm. By contrast, *SIVF* and *IVF-CBICP* executed the same number of the similarity calculations, which corresponded to only 30% to 65% of the baseline. However, there was the large difference between the elapsed times of *SIVF* and *IVF-CBICP* in Fig. 7(a).

We analyzed the *SIVF* speed performance from the viewpoint of DFs. Figure 8(b), (c), and (d) show the characteristics of the DFs; the number of retired instructions, BMs, and LLCMs.

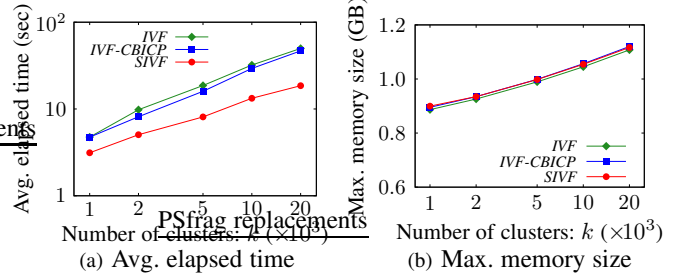


Fig. 7. Performance of three algorithms that were executed by 50-thread processing with given k in 1M-sized PubMed. (a) Average elapsed time per iteration is plotted along k with log-log scale and (b) Occupied maximum memory size through iterations along k with log-linear scale.

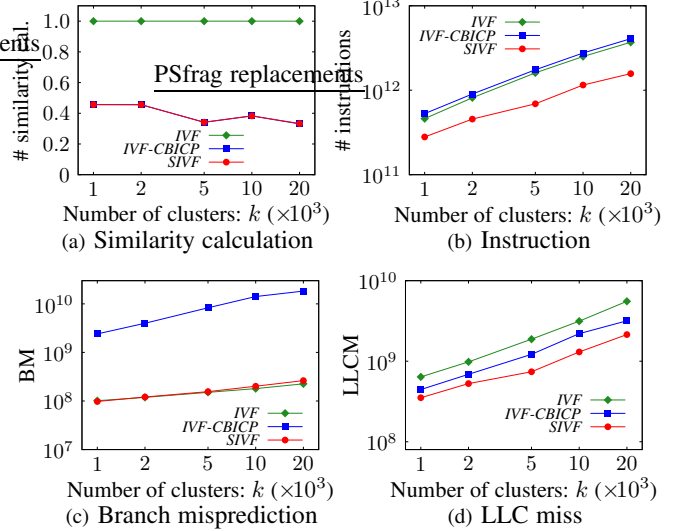


Fig. 8. (a) Number of similarity calculations normalized by $(N \times k)$ and characteristics of performance degradation factors: (b) the number of instructions (Inst), (c) branch mispredictions (BM), and (d) last-level cache misses (LLCM) when the three algorithms were executed by 50-thread processing for 1M-sized PubMed. (a) is plotted with log-linear scale and (b), (c), and (d) with log-log scale.

The number of retired instructions of *SIVF* was smallest in all the k values because of the reduction of instructions for similarity calculations with ICP in Fig. 8(a). In the case of *IVF-CBICP*, positive and negative effects on the number of instructions compensated by decreasing the number of similarity calculations and increasing the number of conditional branches, resulting in the similar characteristics as *IVF*. In Fig. 8(c), *SIVF* reduced the branch mispredictions as much as *IVF* although *IVF-CBICP* caused many branch misprediction. *SIVF* also reduced the last-level cache misses by skipping unnecessary similarity calculations with ICP based on the structured inverted file.

Thus suppressing the DFs as well as reducing the similarity calculations, i.e., exploiting the advantages of the computer architecture, led to the *SIVF*’s high-speed performance.

7 CONCLUSION

We proposed an architecture-friendly structured inverted-file k -means clustering algorithm (*SIVF*) that operated at higher speed and with lower memory consumption in large-scale high-dimensional sparse document data sets when large k values were given, compared with the existing algorithms. Our analysis on the experimental results revealed that *SIVF*’s high-performance came from suppressing the performance degradation factors of

the numbers of cache misses and branch mispredictions rather than decreasing the number of expensive similarity calculations. Our approach of devising a data structure to exploit advantages of computer architecture provides an algorithm design guideline for large-scale and high-dimensional sparse data sets.

There remain the two directions as the future work. One is to clarify the limitations of our algorithm, for instance, on the parameters of k , data size N , the sparsity of an object data set and a mean set, and the characteristics of the object data set like the power-law distribution of appearing terms. The other is to develop more efficient filter that can reduce more similarity calculations instead of the weak ICP and incorporate it into *SIVF* so as to become an architecture-friendly algorithm.

REFERENCES

- [1] S. Marsland, *Machine learning: An algorithmic perspective*. CRC Press, 2015.
- [2] S. Büttcher, C. L. A. Clarke, and G. V. Cormack, Eds., *Information retrieval: Implementing and evaluating search engines*. Cambridge, Massachusetts: The MIT Press, 2010.
- [3] J. Yang, J.-G. Jiang, A. G. Hauptmann, and C.-W. Ngo, "Evaluating bag-of-visual-words representations in scene classification," in *Proc. ACM SIGMM Int. Workshop Multimedia Information Retrieval*, 2007, pp. 197–206.
- [4] J. Sivic and A. Zisserman, "Video Google: A text retrieval approach to object matching in videos," in *Proc. IEEE Int. Conf. Computer Vision (ICCV)*, 2003, pp. 1470–1478.
- [5] B. George and B. Yegnanarayana, "Unsupervised query-by-example spoken term detection using segment-based bag of acoustic words," in *Proc. IEEE Int. Conf. Acoust. Speech Signal Process. (ICASSP)*, 2014, pp. 7133–7137.
- [6] C. C. Aggarwal, *Recommender systems: The textbook*. Springer, 2016.
- [7] J. Kleinberg and E. Tardos, *Algorithm design*. Pearson, Addison Wesley, 2005.
- [8] J. L. Hennessy and D. A. Patterson, *Computer architecture, sixth edition: A quantitative approach*. San Mateo, CA: Morgan Kaufmann, 2017.
- [9] H. Zhang, G. Chen, B. C. Ooi, K.-L. Tan, and M. Zhang, "In-memory big data management and processing: A survey," *IEEE Trans. Knowl. Data Eng.*, vol. 27, no. 7, pp. 1920–1948, 2015.
- [10] M. Evers and T.-Y. Yeh, "Understanding branches and designing branch predictors for high-performance microprocessors," *Proc. IEEE*, vol. 89, no. 11, pp. 1610–1620, 2001.
- [11] S. Eyerly, J. E. Smith, and L. Eeckhout, "Characterizing the branch misprediction penalty," in *Proc. IEEE Int. Symp. Perform. Anal. Syst. Softw. (ISPASS)*, 2006, pp. 48–58.
- [12] S. Chen, A. Ailamaki, P. B. Gibbons, and T. C. Mowry, "Improving hash join performance through prefetching," *ACM Trans. Database Syst.*, vol. 32, no. 3, pp. 1–32, 2007.
- [13] X. Wu, V. Kumar, J. R. Quinlan, J. Ghosh, Q. Yang, H. Motoda, G. J. McLachlan, A. Ng, B. Liu, P. S. Yu, Z.-H. Zhou, M. Steinbach, D. J. Hand, and D. Steinberg, "Top 10 algorithms in data mining," *Knowl. Inf. Syst.*, vol. 14, no. 1, pp. 1–37, 2008.
- [14] G. Hamerly and J. Drake, "Accelerating Lloyd's algorithm for k-means clustering," in *Partitional Clustering Algorithms*, M. E. Celebi, Ed. Springer, 2015, ch. 2, pp. 41–78.
- [15] S. P. Lloyd, "Least squares quantization in PCM," *IEEE Trans. Information Theory*, vol. 28, no. 2, pp. 129–137, 1982.
- [16] J. B. MacQueen, "Some methods for classification and analysis of multivariate observations," in *Proc. 5th Berkeley Symp. Mathematical Statistics and Probability*, 1967, pp. 281–297.
- [17] I. S. Dhillon and D. S. Modha, "Concept decompositions for large sparse text data using clustering," *Machine Learning*, vol. 42, no. 1–2, pp. 143–175, 2001.
- [18] Perf, "Linux profiling with performance counters," 2019. [Online]. Available: <https://perf.wiki.kernel.org/index.php>
- [19] C. Elkan, "Using the triangle inequality to accelerate k-means," in *Proc. 20th Int. Conf. Machine Learning (ICML)*, 2003, pp. 147–153.
- [20] G. Hamerly, "Making k-means even faster," in *Proc. SIAM Int. Conf. Data Mining (SDM)*, 2010, pp. 130–140.
- [21] J. Drake and G. Hamerly, "Accelerated k-means with adaptive distance bounds," in *Proc. 5th NIPS Workshop on Optimization for Machine Learning*, 2012.
- [22] Y. Ding, Y. Zhao, X. Shen, M. Musuvathi, and T. Mytkowicz, "Yinyang k-means: A drop-in replacement of the classic k-means with consistent speedup," in *Proc. 32nd Int. Conf. Machine Learning (ICML)*, 2015, pp. 579–587.
- [23] J. Newling and F. Fleuret, "Fast k-means with accurate bounds," in *Proc. 33rd Int. Conf. Machine Learning (ICML)*, 2016.
- [24] T. Hattori, K. Aoyama, K. Saito, T. Ikeda, and E. Kobayashi, "Pivot-based k-means algorithm for numerous-class data sets," in *Proc. SIAM Int. Conf. Data Mining (SDM)*, 2016, pp. 333–341.
- [25] K. Aoyama, K. Saito, and T. Ikeda, "Accelerating a Lloyd-type k-means clustering algorithm with summable lower bounds in a lower-dimensional space," *IEICE Trans. Inf. & Syst.*, vol. E101-D, no. 11, pp. 2773–2782, 2018.
- [26] T. Kaukoranta, P. Fränti, and O. Nevalainen, "A fast exact GLA based on code vector activity detection," *IEEE Trans. Image Process.*, vol. 9, no. 8, pp. 1337–1342, 2000.
- [27] T. Bottesch, T. Bühler, and M. Kächele, "Speeding up k-means by approximating Euclidean distances via block vectors," in *Proc. 33rd Int. Conf. Machine Learning (ICML)*, 2016.
- [28] H. Samet, Ed., *Foundations of multidimensional and metric data structures*. San Francisco, CA, USA: Morgan Kaufmann Publishers Inc., 2006.
- [29] D. Harman, E. Fox, R. Baeza-Yates, and W. Lee, "Inverted files," in *Information retrieval: Data structures & algorithms*, W. B. Frakes and R. Baeza-Yates, Eds. New Jersey: Prentice Hall, 1992, ch. 3, pp. 28–43.
- [30] D. E. Knuth, "Retrieval on secondary keys," in *The art of computer programming: Volume 3: Sorting and searching*. Addison-Wesley Professional, 1998, ch. 5.2.4 and 6.5.
- [31] J. Zobel and A. Moffat, "Inverted files for text search," *ACM Computing Surveys*, vol. 38, no. 2, article 6, 2006.
- [32] A. Broder, L. Garcia-Pueyo, V. Josifovski, S. Vassilvitskii, and S. Venkatesan, "Scalable k-means by ranked retrieval," in *Proc. ACM Int. Conf. Web Search and Data Mining (WSDM)*, 2014, pp. 233–242.
- [33] K. Aoyama, K. Saito, and T. Ikeda, "Inverted-file k-means clustering: Performance analysis," *arXiv preprint arXiv:2002.09094*, 2020.
- [34] Y. LeCun and C. Cortes, "MNIST handwritten digit database," 2010. [Online]. Available: <http://yann.lecun.com/exdb/mnist>
- [35] A. Torralba, R. Fergus, and W. T. Freeman, "80 million tiny images: A large data set for nonparametric object and scene recognition," *IEEE Trans. Pattern Anal. Mach. Intell.*, vol. 30, no. 11, pp. 1958–1970, 2008.
- [36] D. Dua and E. K. Taniskidou, "Bag of words data set (PubMed abstracts) in UCI machine learning repository," 2017. [Online]. Available: <http://archive.ics.uci.edu/ml>
- [37] P. Hammarlund, A. J. Martinez, A. A. Bajwa, D. L. Hill, E. Hallnor, H. Jiang, M. Dixon, M. Derr, M. Hunsaker, R. Kumar, R. B. Osborne, R. Rajwar, R. Singhal, R. D'Sa, R. Chappell, S. Kaushik, S. Chennupati, S. Jourdan, S. Gunther, T. Piazza, and T. Burton, "Haswell: The fourth-generation Intel core processor," *IEEE Micro*, vol. 34, issue 2, pp. 6–20, 2014.
- [38] OpenMP, "The OpenMP API specification for parallel programming," 2021. [Online]. Available: <https://www.openmp.org>
- [39] R. Jongerius, A. Anghel, G. Dittmann, G. Mariani, E. Vermij, and H. Corporaal, "Analytic multi-core processor model for fast design-space exploration," *IEEE Trans. Comput.*, vol. 67, no. 6, pp. 755–770, 2018.
- [40] A. Yasin, "Top-down method for performance analysis and counters architecture," in *Proc. IEEE Int. Symp. Perform. Anal. Syst. Softw. (ISPASS)*, 2014, pp. 35–44.

APPENDIX A

PERFORMANCE COMPARISON RESULTS IN NYT

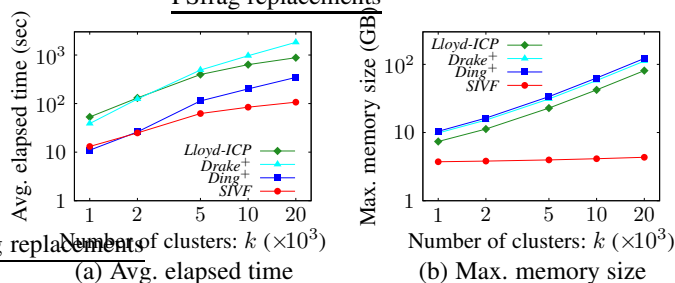


Fig. 9. Performance of four algorithms executed by 50-thread processing with given k in NYT. (a) Average elapsed time per iteration and (b) Occupied maximum memory size through iterations were plotted along k with log-log scale.

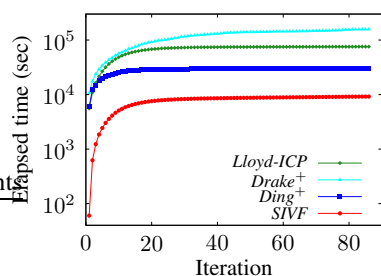


Fig. 10. Elapsed time that four algorithms with $k=20,000$ required until convergence when they were applied to NYT. Elapsed time is plotted along iteration with linear-log scale.

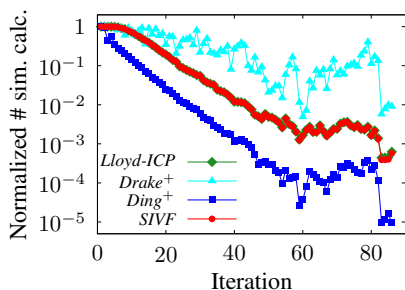


Fig. 11. Number of similarity calculations normalized by $(N \times k)$, where N indicates the data size of 1,285,944, when four algorithms with $k=20,000$ were executed by 50-thread processing for NYT. Normalized number is plotted along iteration with linear-log scale.

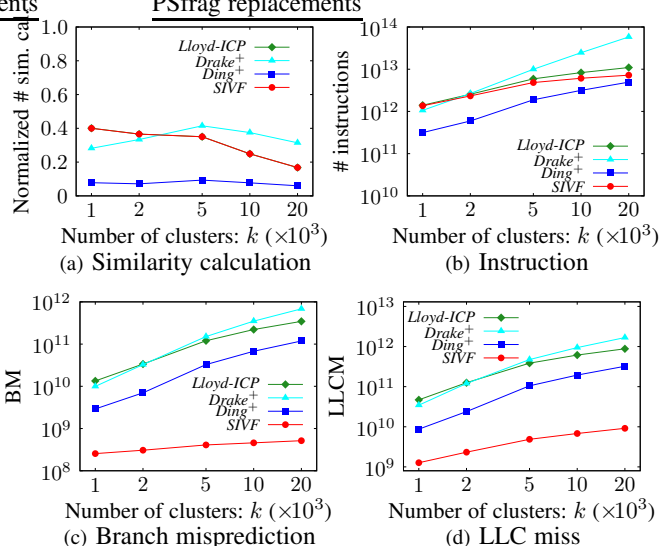


Fig. 12. (a) Number of similarity calculations normalized by $(N \times k)$ and characteristics of performance degradation factors: (b) the number of instructions (Inst), (c) branch mispredictions (BM), and (d) last-level cache misses (LLCM) when the three algorithms were executed by 50-thread processing for NYT. (a) is plotted with log-linear scale and (b), (c), and (d) with log-log scale.